Analysis of the Native Structure of Starch Granules with X-ray Microfocus Diffraction

Thomas A. Waigh, Ian Hopkinson, and Athene M. Donald*

Cavendish Laboratory, Madingley Road, Cambridge CB3 OHE, England

Michael F. Butler

Department of Material Science and Metallurgy, New Museum Site, Cambridge, CB2 3QJ, England

Florian Heidelbach and Christian Riekel

ESRF, B.P. 220, F-38043 Grenoble, France

Received January 22, 1997; Revised Manuscript Received March 28, 1997[⊗]

ABSTRACT: Results of microfocus X-ray diffraction at the ESRF are presented which provide unique evidence supporting a model for the structure of starch, much of this model having been previously derived only on the basis of circumstantial evidence. Here we present data from ∼2 μm regions within granules which have been subjected to no sample preparation and obtain oriented 2-D fiber patterns from the edge of B-type potato starch granules. This data is in good agreement with that previously calculated by Imberty/Perez[1] for a B-type amylose fiber. The peripheral amylopectin helices are oriented in such a way they do not point to a single focus. No discontinuities ("grain boundaries") within a granule could be found at the 10 μm level of resolution.

Introduction

The supramolecular structure of starch remains a puzzle within the field of plant molecular biology. Genetic engineering is beginning to produce starches with novel supramolecular architectures as the enzymes in the cultivar's metabolic pathway may now be altered.[2] These new products could be of crucial industrial importance, but even the structures of wild-type starches are not well understood.

Sample preparation has provided the foremost problem facing the complete structural elucidation of starch in its native form. Electron microscopy requires the production of microtomed sections and additionally requires samples to be examined under vacuum. It is thus liable to affect the native structure of the granule which in turn leads to problems with interpretation.[3,4] An extremely detailed model of starch has been proposed by Oostergetel et al.[5] in 1993 using tomographic reconstruction of transmission electron micrographs, but has as yet received no corroboration from other techniques. It appears likely that microfocus X-ray diffraction will eventually provide this required information as outlined in the Future Work section. Microfocus X-ray diffraction will also always have the advantage over electron diffraction that the kinematic approximation can be used to analyze the data.[6] Difficult multiple scattering calculations do not have to be made (the dynamic approximation), since the X-rays interact much more weakly with matter than electrons.

The conventional model of starch is that it is formed from three regions, crystalline and amorphous lamellae, which together form the crystalline growth ring, and amorphous growth rings,[7] as shown in Figure 1. The largest granules presented by nature are those found in potato tubers. These are elliptical in shape with their longest axis on the order of 100 μm.[8] Previous X-ray diffraction experiments have thus been restricted to measurements averaging over many granules[9−11] (e.g. at the Daresbury synchrotron source, using beam lines 2.1 and 8.2) with a typical beam size of a few millimeters, yielding a powder average, but with no knowledge of the ordering of the crystallites within a granule. In this paper we present scans of a 2 μm X-ray beam across a native granule. Diffraction patterns have been obtained at 10 μm steps across one granule from potato starch.

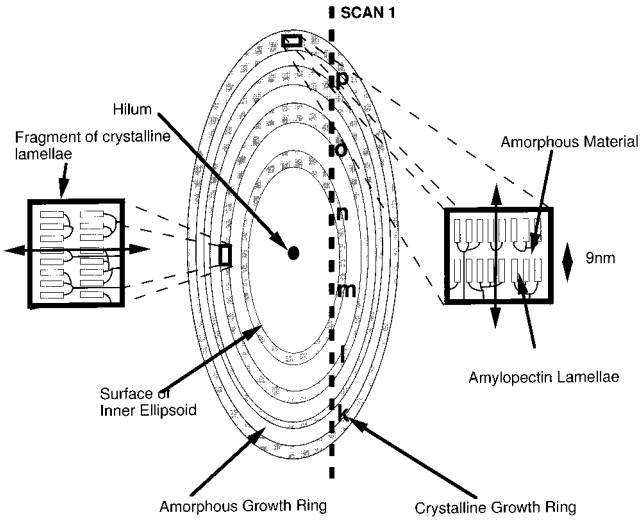

Figure 1. Granule in cross section showing the orientation of amylopectin double helices in the crystalline lamellae (not to scale). Scan 1 shows the path followed to obtain the diffraction patterns showed in Figure 6.

The point of initiation of the granule is called the hilum. It can be found near the center of elliptical granules or positioned on the axis of symmetry, at the fat end of pear-shaped granules. It is usually considered to be less well organized than the rest of the granule, although few details are known on its exact organization and composition.[12]

It is postulated that the amylopectin lamellae in potato starch are arranged in the B-type crystalline

* To whom correspondence should be addressed.
[⊗] Abstract published in *Advance ACS Abstracts,* June 1, 1997.

S0024-9297(97)00075-2 CCC: $14.00

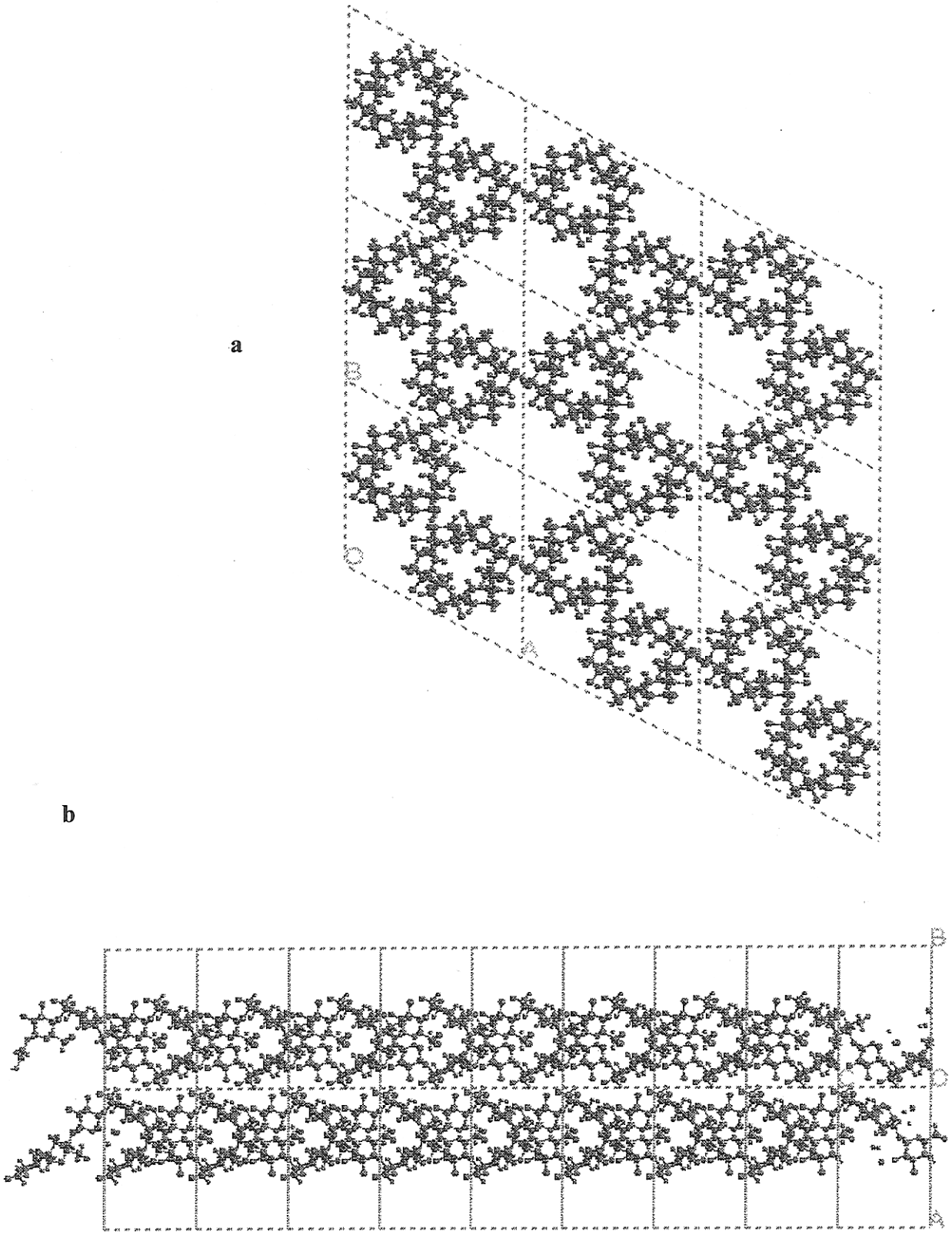

Figure 2. Crystalline structure of B-type starch as calculated from the unit cell of Imberty.[1] The (001) and (110) planes, a and b, respectively, are shown.

form. This consists of a hexagonal unit cell, space group $P6_1$, lattice parameters $a = b = 18.5$ Å and $c = 10.4$ Å, taking the unit cell of Perez[1](Figure 2). Refinements of this structure have been achieved using amylose fibers, and by comparison with powder diffraction data, it is concluded that a similar structure occurs in the native granule.[13−15]

The hydration of B-type starch also provides an interesting phenomenon. The addition of water has significant effect on its structure. Previously, based on results from small and wide angle X-ray scattering.[16] we have put forward a model for the self-assembly of amylopectin lamellae during hydration.[17] Water plasticizes the amorphous lamellae and allows the amy-

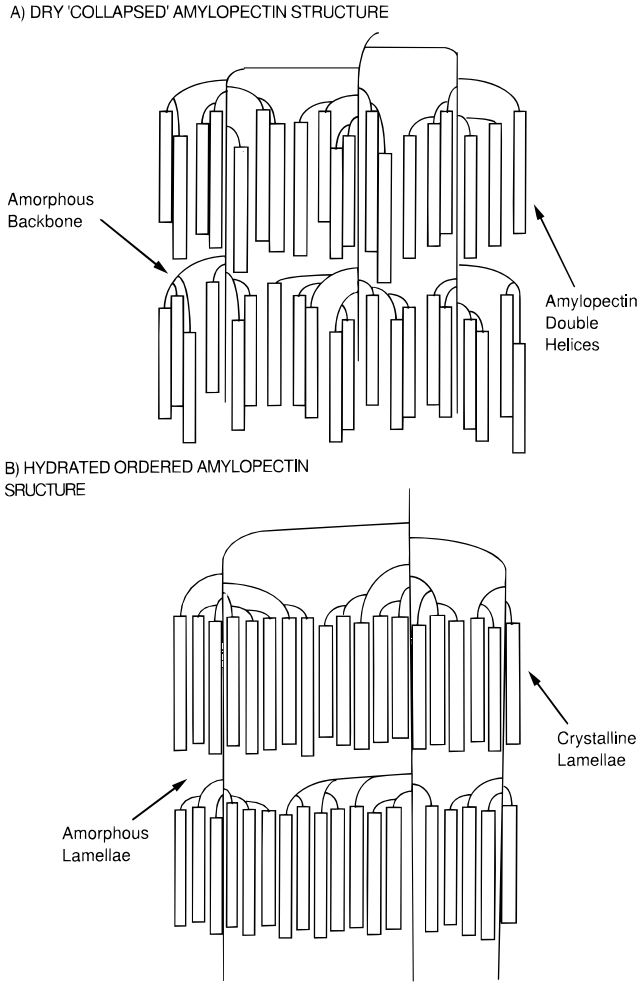

Figure 3. Cartoon indicating the processes involved during the hydration of potato starch. The unit cell is not well depicted.

lopectin helices to organize side by side in a smectic A type structure[18] (Figure 3). In the present paper we briefly consider the effect of water on the fiber patterns obtained from the periphery of potato granules.

Sample Preparation

Potato samples were obtained from Sigma. Wheat (with diameters of ~30−40 μm), barley (30−40 μm), plantain (60 μm), and banana (60 μm) starches were gifts from Dr Mike Gidley, Unilever Colworth. Only potato produced strong enough diffraction patterns to be usefully recorded, however. With the other samples we only gained information concerning the nature of the beam damage.

Sample mounting was an extremely delicate process. The carbon film necessary to support the granules needed to be extremely thin (less than 1 μm) in order for it to create negligible background scattering compared with the weakly scattering granules. Starch was sieved and centrifuged to provide the largest available granules from each cultivar. Next, under a stereomicroscope, a bubble of water was placed onto the carbon support film (purchased from Agar Scientific), which had a copper locator grid glued on its other side, as shown in Figure 4a. The locator grid had a 500 μm hole punched in it. The presence of this hole permits the collection of diffraction data without the problem of copper peaks obscuring the data. Next a small number of granules were dropped into the bubble with an eyelash brush. For the smaller granules an acetone/water mixture had to be used to be added to the granules to prevent aggregation. Slowly, by carefully monitoring the buildup in the microscope, a monolayer of starch could be produced on the carbon film. Natural evaporation was allowed to remove most of the excess water,

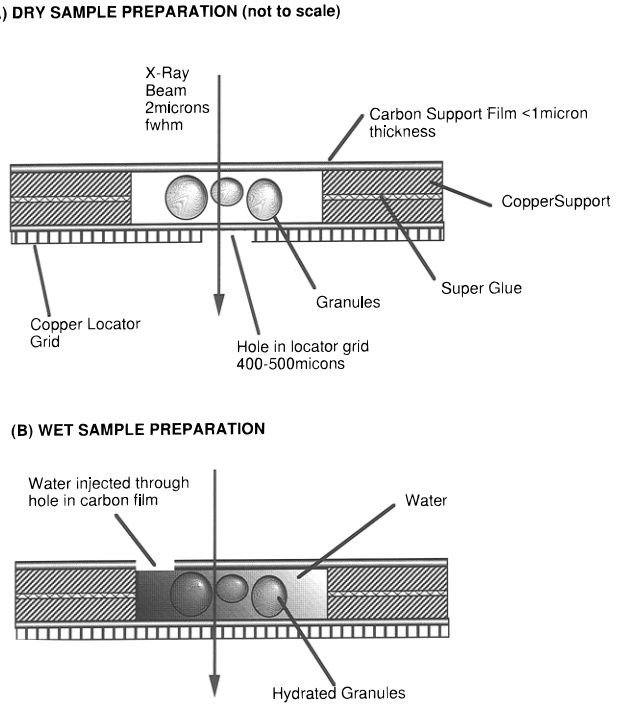

Figure 4. Two modes of sample preparation of dry/hydrated starch.

and the sample was immediately sealed with another (upper) grid mounted support film. Estimation of the water content of such minute samples is hazardous, but limiting water levels are on the order of 30% w/w (water/starch), and it is assumed that these "dry" samples have less water than this.

High water content samples (ca. 45% w/w) were prepared by piercing the upper carbon film. When the cell was floated in water and a bubble of water was placed on top of the pierced hole, water was sucked through the hole into the cell by capillary action, hydrating the sample (Figure 4b).

The final samples were embedded directly in wax, which also served as a calibration standard, on the goniometer head, and this was placed within a millimeter of the tip of the glass capillary used in the final stage of X-ray focusing.

Experimental Section

The beam was collimated with a glass capillary to achieve a 2 μm full width at half-maximum. The 13 keV (0.954 Å) X-rays were incident on the sample. The beam divergence at the exit of the glass capillary was 2.3 mrad, and the sample was placed 1 mm away from it. Flux at the sample was 10×10^{10} ph/s. A more detailed account of the beam line set up may be found in Engström et al.[19,20] Calibration in 2θ was achieved using a wax standard, since it is used as a sample support material, and its diffraction patterns may thus be obtained for a specific geometry without replacing the sample or entering the hutch. For data display and data reduction the software package FIT2D was used.[21] The spatial distortions on the CCD detector were corrected with a standard grid file supplied by Dr. Engström (ESRF).

Beam damage occurred very rapidly with all the samples, diffraction patterns being lost after around 10 s. This problem was in one respect an advantage, however, as it provided a background count for each region which could then be subtracted from the data, allowing the separation of the sample scattering from that of the shadow of the copper grid. Potato starch was more resistant to X-ray induced disruption, by a factor of 10, over the other starches examined: wheat, barley, banana, and plantain (unit cell types A, A, C, and C, respectively). Beam damage between separate granular areas was judged to be negligible, since there is no decrease in the intensity of the measured diffraction patterns at neighboring positions on one granule separated by 10 μm. This null result required verification since thermal conduction or the skirt of

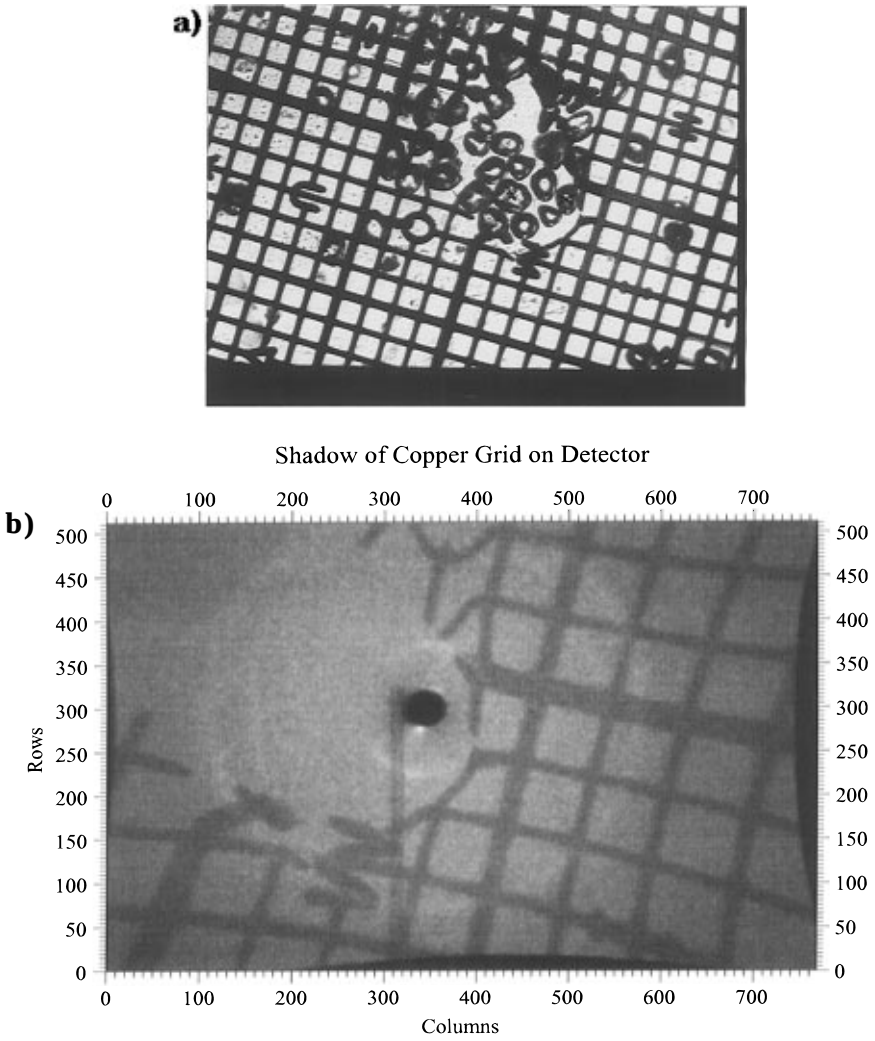

Figure 5. Location of starch granules in the beam: (a) optical photograph of the prepared sample; (b) plot of the corresponding data collected on the CCD camera. The shadow of the copper grid and the beam stop can be seen in part b.

the collimated beam could have been causing nonlocal damage to the sample.

Individual granules were located by photographing the cell under an optical microscope before mounting on the goniometer head (Figure 5a) and matching this with a shadow of the copper locator grid on the X-ray detector (Figure 5b).

To minimize the rate of beam damage on wheat, we attempted to reduce the flux of the beam by mis-aligning the glass capillary. The more obvious solution of placing a piece of lead in the sealed optical system upstream of the capillary was not used since the required thickness of attenuator was not available. The misalignment procedure was a poor solution to the problem, however, since it caused the intensity of flux to oscillate every minute (the beam oscillated with a period of 10 min otherwise), leading to subsequent problems in background subtraction.

Order Parameters

Order parameters offer an elegant method of quantifying the degree of orientation displayed by a particular reflection (as previously used in this context by Zachmann et al.[22]). Following the method of Windle,[23,24] we shall describe the amount of misorientation (assumed cylindrically symmetric) of the double helices away from their mean axis, by expressing D(α) as a sum of Legendre polynomials $P_{2n}(\cos\alpha)$.

$$D(\alpha) = \sum_{n=0}^{\infty} (4n + 1)\langle P_{2n}(\cos\alpha)\rangle P_{2n}(\cos\alpha) \qquad (1)$$

Experimentally values of the Legendre polynomial weightings may be calculated from an azimuthal scan of the diffraction pattern through

$$\langle P_{2n}(\cos\alpha)\rangle = \frac{\int_0^{\pi/2} I(s,\alpha)P_{2n}(\cos\alpha)\sin\alpha\, d\alpha}{\int_0^{\pi/2} I(s,\alpha)\sin\alpha\, d\alpha} \qquad (2)$$

where s is a constant radial reciprocal lattice polar coordinate, α is the variable azimuthal polar coordinate, and $I(s,\alpha)$ is the intensity of a particular reflection. The transformation to polar co-ordinates was achieved using the r/θ rebinning routine in Fit2D.

Results

Many linear scans were achieved across moist (~30% w/w) and wet (~45% w/w) potato granules for a variety of granule sizes. A representative example may be seen in Figure 6 for wet starch, which shows six patterns taken at 10 μm steps across a granule at the positions shown in Figure 1. To improve the signal/noise ratio of the diffraction patterns, frame averaging between similar locations on separate granules was used. In practice, averaging was achieved by using Fit2D to rotate similarly well-resolved patterns into register and then adding them. Granules were also quadrant averaged to achieve a 2-fold improvement in signal to noise.

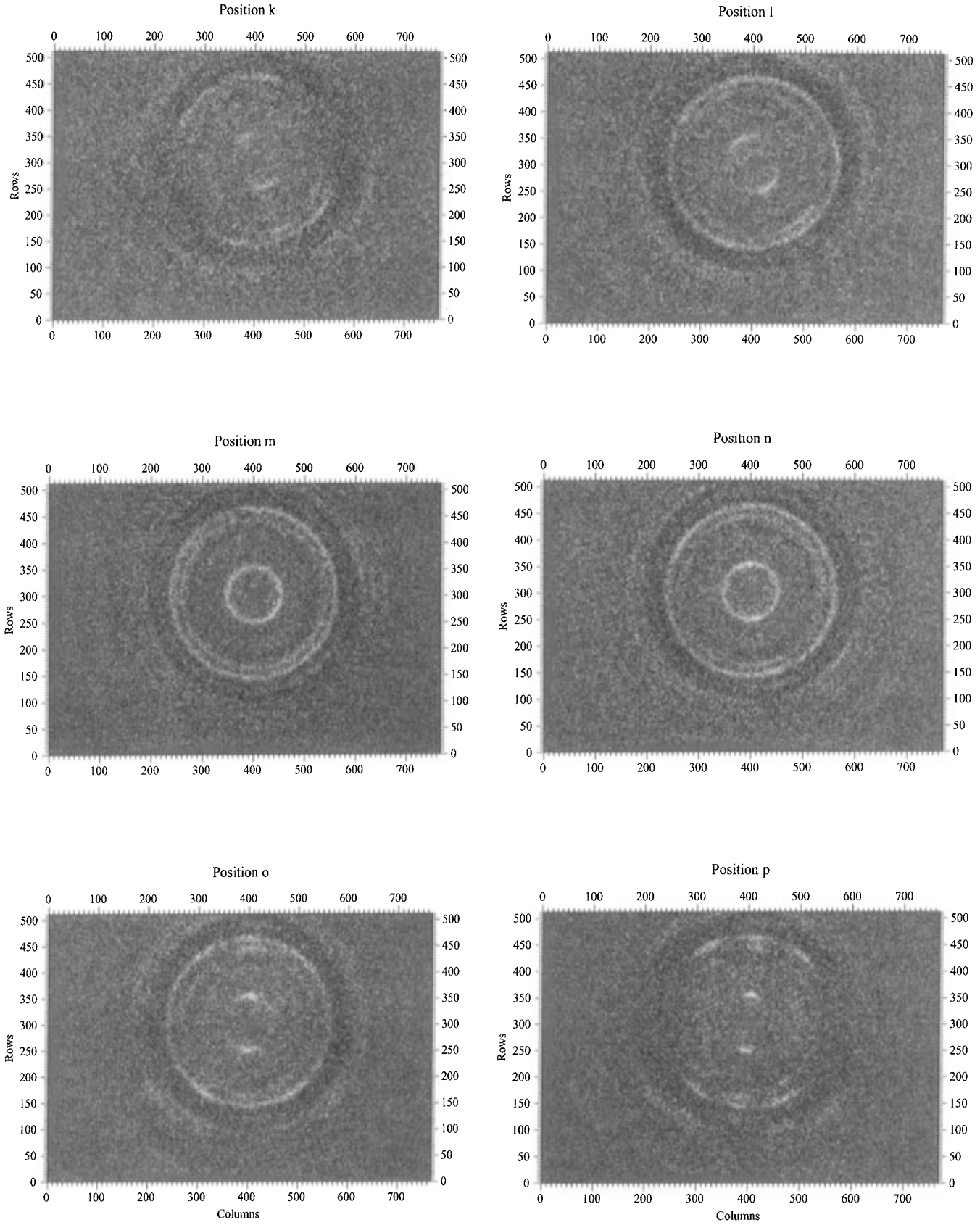

Figure 6. Linear scan through a single wet potato granule showing microfocus patterns taken at 10 μm steps. Positions on the granule are marked on Figure 1.

Figure 7a shows a diffraction pattern averaged over similar peripheral positions on four similarly sized wet granules. It should be noted, however, that raw data were always used to deduce the alignment of amylopectin helices (as in Figure 6, from which Figure 10 is derived), and for any determination of orientation order parameters. For comparison with Figure 7a, the fiber diffraction pattern of the unit cell of Imberty/Perez[1] was calculated using Cerius. Graphical output from this program is shown in Figure 7b. A Gaussian misorien-

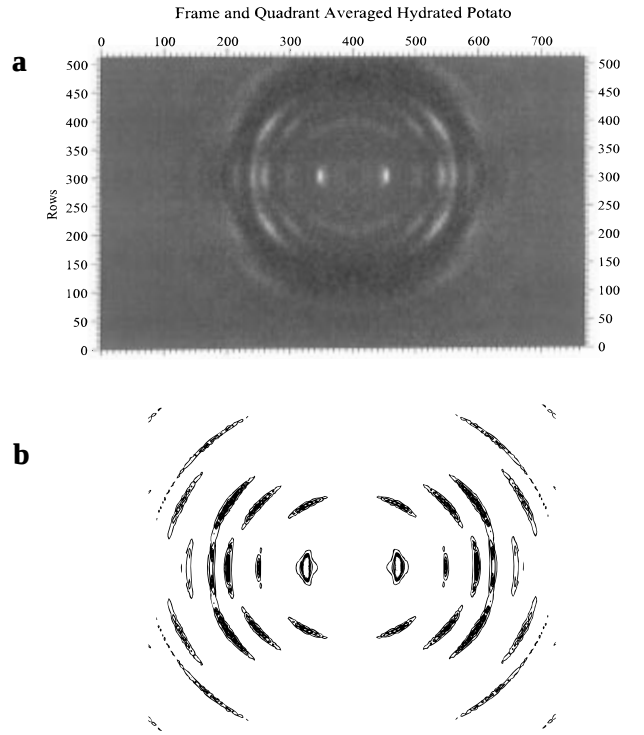

Figure 7. Comparison of fiber diffraction patterns: (a) a frame averaged microdiffraction pattern obtained from the edge of wet potato granules compared with (b) the pattern calculated with Cerius from the unit cell of Imberty.[1]

tation function of full width at half-maximum of 8° had to be assumed to achieve agreement with the data. Comparison of the patterns indicates a good match between the two images, although the paucity of reflections stops us from doing any reliable integration of the diffraction patterns and calculations of R factors.[25]

In the present experiment we used the (100) interhelix peak (the closest reflections left and right of the beam stop, as for instance visible in Figure 7b) to calculate Legendre polynomials according to eq 2. The value of P_2 calculated for the edge of wet potato (corresponding to excess water at around 45% w/w, and shown in Figure 8a) is 0.53, and it is 0.46 for dryer potato (limiting water ~30% w/w Figure 8b), using similarly sized granules. We must however take these results as preliminary in nature since they were achieved through integration over azimuthal scans with significant levels of noise. Such an analysis is also not completely valid for the asymmetric patterns collected from starch, as cylindrical symmetry is assumed. The lack of 4-fold rotational symmetry found in some of the measured diffraction patterns is probably due to there being different path lengths for different trajectories of the scattered X-rays through the elliptical granule, which in turn produce different degrees of attenuation. The calculation of order parameters is also affected by the projection of the radially arranged amylopectin helices sampled by the beam. Only at the edge is this projection across well-oriented fibers, producing high-order parameters. Toward the center of the granule the beam will average over helices pointing forward, backward, and sideways, reducing the value of the order parameter and complicating its interpretation.

An extremely weak diffraction pattern obtained for hydrated wheat is shown in Figure 9. The collection time was increased from 10 to 50 s since there was a 5-fold decrease in flux after capillary misalignment. Thus, although the total integrated flux remained constant, the rate of dissipation of energy in the sample decreased, and this appears to be critically important for sample stability.

Discussion

A representative linear scan for 10 μm steps across a potato granule was obtained (Figure 6), and the appropriate positions of these are marked on Figure 1 based on the use of the optical micrograph/locator grid cross-reference. By analysis of the direction of the (100) peaks (the interhelical reflections), the orientation of the double helices in the granule could be deduced. They may be seen not to point toward a single focus. Although with the limited number of data points available exactly how the orientation varies all the way around a granule is not clear, the data are consistent with the helices pointing toward the surface of an inner ellipsoid (Figure 10). The helices are also found to be perpendicular to the surface of the granule; i.e., they are radially oriented. This is in agreement with information derived from birefringence studies,[26] which indicate a similar result although in a less direct manner (assumptions have to be made about the correlation between the principal optic axis and the molecular axis[8]). There were no discontinuities of orientation (disclinations or grain boundaries) discovered at the 10 μm level; i.e., there was a gradual change in the direction of the helices between 10 μm steps, consistent throughout with radial orientation of the helices.

Hydration causes the peaks to both increase in intensity and sharpen (increase in P_2), as can be seen in Figure 8. From previous studies (ref 17, see Figure 3), we deduce that the amylopectin double helices (mesogens) are moving into register in their smectic A type structure upon the addition of water and that this causes the increase in peak intensity since the periodicity of the packing has been improved. Furthermore we can postulate that the increase in P_2 is specifically due to the helices becoming less splayed during their hydration; i.e., they tend to line up along some common axis. It must be noted however that values of P_2 are critically sensitive to the amount of material sampled, i.e. the beam size and the thickness of the material. P_2 values increase as the beam size is decreased, if there is a constant helix−helix correlation. Thus we can only make these qualitative deductions on P_2 data specifically obtained from the edge (±5 μm) of large (~60−100 μm) potato starch granules with a 2 μm beam.

The B type[10] fiber diffraction pattern observed (following averaging) at the edge of the potato granule (Figure 7a) shows very good agreement with the unit cell of Imberty/Perez (Figure 7b). There does however appear to be an anomalous blurring of peaks on the first layer line above and below the (100). Explanation of this result will need to await improved data sets. The position of the (100) peaks (representative of the interhelical distance) in potato starch did not change upon increased hydration, and there was no variation with the distance from the center of the granule.

The rate of beam damage in the A and C type unit cell starches studied is an order of magnitude above that of potato starch. The amylopectin double helices are longest in potato starch,[27] and it may be this factor which increases their stability. The extra length of helix may tend to pin the amylopectin chains in their crystalline unit cells as the X-rays disrupt the molecular bonding. Alternatively, the extra water available in the B-type unit cell may provide a more efficient loss

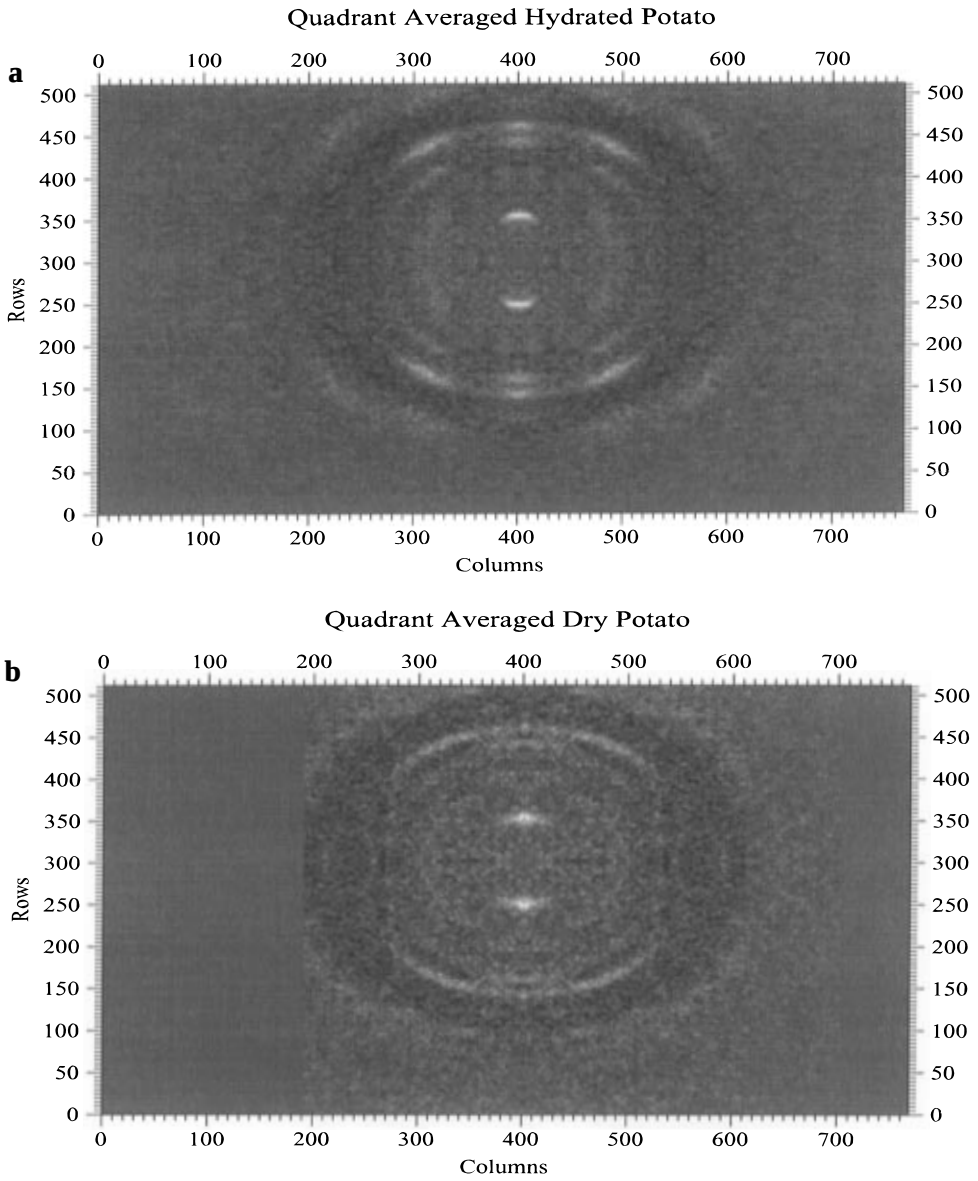

Figure 8. Comparison of representative microdiffraction patterns from the edge of (a) wet granules (~45% w/w) and (b) moist granules (~30% w/w).

mechanism for the X-rays' energy. A weak wheat pattern was obtained on misaligning the glass capillary. The strongest diffraction pattern achieved showed a little orientation in the quadrant averaged image, Figure 9, though few conclusions should be drawn on such a weak data set. Very faint diffraction patterns were obtained for plantain and banana starches, and they yielded no useful information.

There is an extremely large literature on the mechanisms of beam damage with electron microscopy and how to avoid it.[28] Such a detailed range of study must be performed with microfocus X-ray diffraction in order for the technique to realize its true potential.

Future Work

The main obstacle to be overcome for better resolved fiber patterns to be collected is that of beam damage. The prognosis is good, however. Experiments on spider silk have shown that freezing the samples in a nitrogen stream causes a 60-fold increase in the beam stability.[29] Similar improvements should be possible with starch. The signal to noise ratio could also be increased through optimization of the flux at the sample with the correct thickness of attenuator. It is thus quite possible that good quality fiber diffraction patterns may be obtained from starch cultivars other than potato, i.e. wheat, banana, barley, and plantain.

Collecting data over a large number of granules and then averaging over patterns within a definite range of order parameter will achieve a $N^{1/2}$ improvement in the ratio of signal to noise. The optimum solution of this problem would require an optical microscope on the beam line to facilitate completely automatic acquisition of the data, hence increasing collection rates. A carefully calibrated optical microscope could also allow for the removal of the copper locator grid and the related problem of background subtraction.

Once better resolved peaks are achieved a serious effort can be made to model the degree of axial tilt of the fibrous assembly (currently assumed to be cylindrically symmetric) in the granule and the disorder in the diffraction patterns.[30,31,32]

A much more advanced model for the supermolecular structure of starch has been put forward by Oostergetel[5] on the basis of tomographic reconstruction of electron micrographs. This consists of a complicated superhe-

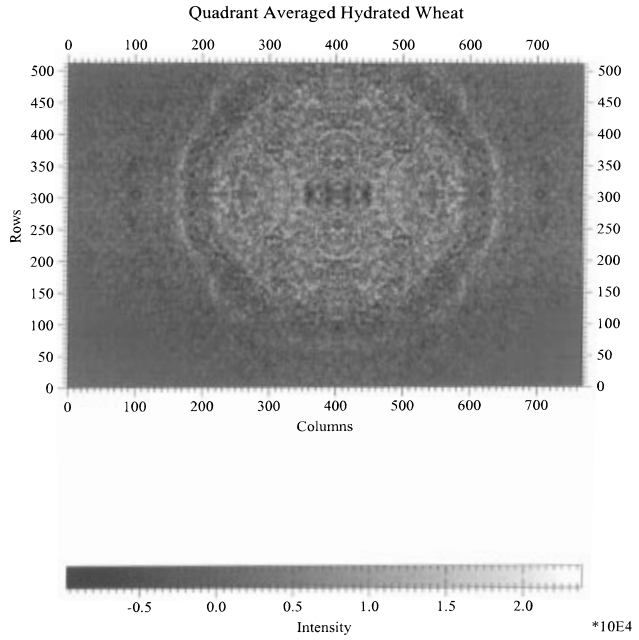

Figure 9. Weak microdiffraction pattern from wheat showing orientation.

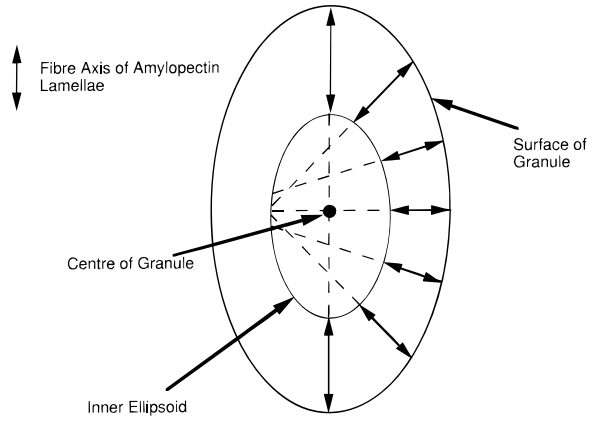

Figure 10. Schematic diagram showing the orientation of amylopectin helices in a plane cross section through a potato starch granule. The fiber axes are perpendicular to an inner elipsoid.

lical array of the amylopectin lamellae, the synthesising enzyme being assumed to move down the hole in the center of the superhelix. The facility of microfocus small-angle X-ray scattering[33] is now available at the 20 μm level, which should enable a rigorous test for the model. Though the sample must be frozen, which is known[34] to reduce the lateral coherence length of the lamellae by a factor of 4−5 at −30 °C (reducing the peak height by this amount), when this is set against the improved stability in the beam, it is still a worthwhile experiment. If an amylopectin lamellar motif is attached to the paracrystalline helical structure factor of Innouye et al.[35] a cross pattern is predicted for the small-angle peaks, whose axis is tilted 90° with respect to the (100) wide-angle peaks.

Acknowledgment. Many thanks to Alain Buléon (INRA, Nantes, France) for help concerning sample preparation, Brad Thiel for help with Cerius, Stuart Clarke for his Legendre polynomial program, Mike Gidley and Martine Debet (Unilever Colworth) for helpful discussions concerning the self-assembly of amylopectin lamellae during hydration, the BBSRC for funding T.A.W, and Andy Hammersley at the ESRF for supplying his Fit2d V7.37 software for analysis of 2-D CD detector data. Cerius is a commercial package produced by Biosym/Molecular Simulations.

References and Notes

(1) Imberty, A.; Perez, S. *Carbohydr. Polym.* **1988**, *27*, 1205−1221.
(2) Ring, S. *Chem. Br.* **1995**, 303−307.
(3) Yamaguchi, M.; Kainuma, K.; French, D. J. *J. Ultrastruct. Res.* **1979**, *69*, 249−261.
(4) Kassenbeck, P. *Starch* **1978**, *30*, 40.
(5) Oostergetel, G. T.; van Bruggen, E. F. J. *Carbohydr. Polym.* **1993**, *21*, 7−12.
(6) Spence, J. C. H.; Zuo, J. M. *Electon Microdiffraction*; Plenum Press: New York, 1992.
(7) Jenkins, P. J.; Cameron, R. E.; Donald, A. M.; Bras, A. M.; Derbyshire, G. E.; Mant, G. R.; Ryan, A. J. *J. Polym. Sci., Part B: Polym. Phys.* **1994**, *32*, 1579−1583.
(8) Blanshard, J. M. V. In *Starch Properties and Potential*; Galliard, T., Ed.; John Wiley & Sons: New York, 1987.
(9) There has been one previous work by Kreger (Kreger, D. R. *Biochim. Biophys. Acta* **1951**, 6, 406), who obtained badly resolved fiber patterns from potato starch using a microcamera and a lab-based X-ray source. This allowed him to make a few general predictions on the unit cell of the granule.
(10) Katz, J. R.; van Itallie, T. B. Z. *Phys. Chem.* **1930**, *150*, 90−99.
(11) Hizukuri, S.; Kaneko, T.; Takeda, Y. *Biochem. Biophys. Acta* **1983**, *760*, 188−191.
(12) French, D. In *Starch Chemistry and Technology*; Whistler, R. L., BeMiller, J. N., Paschall, E. F., Eds.; Academic Press: New York, 1984; pp 188-189.
(13) Imberty, A.; Buleon, A.; Tran, V.; Perez, S. *Starch* **1991**, *43*, 375−384.
(14) Blackwell, J.; Sarko, A.; Marchessault, R. H. *J. Mol. Biol.* **1969**, *42*, 379−383.
(15) Wu, H.; Wu, C. H.; Sarko, A. *Carbohydr. Res.* **1978**, *61*, 7−25.
(16) Unpublished ^{13}C NMR data of Mike Gidley, Unilever, Colworth, England, also appears to be in agreement with the model.
(17) Waigh, T. A.; Jenkins, P. J.; Donald, A. M. *Faraday Discuss.* **1996**, *103*, 325−337.
(18) Donald, A. M.; Windle, A. H. *Liquid Crystalline Polymers*; Cambridge University Press: Cambridge, England, 1992.
(19) Engstrom, P.; Fiedler, S.; Riekel, C. *Rev. Sci. Instrum.* **1995**, *66*, 1348−1351.
(20) Engstrom, P.; Riekel, C. *J. Synchrotron Radiat.* **1996**, *3*, 97−100.
(21) Hammersley, A.; Svensson, S.; Thompson, A. *Nucl. Instrum. Methods* **1994**, *A346*, 312.
(22) Dreher, S.; Zachmann, H. G.; Riekel, C.; Engstrom, P. *Macromolecules* **1995**, *28*, 7071−7074.
(23) Windle, A. H. In *Developments in Crystal Polymer I*; Ward, I. M., Ed.; Applied Science Publishers: Oxford, England, 1982.
(24) Mitchell, G. R.; Windle, A. H. In *Developments in Crystalline Polymers II*; Bassett, D. C., Ed.; Elsevier Applied Science: Oxford, England, 1988.
(25) R. Denny's advanced fiber diffraction integration software package LSQINT requires on the order of 500 reflections for a simulated annealing Bragg fitting. Denny, R. *Daresbury's CCP13 newsletter*, 2nd ed. 1993.
(26) Banks, W.; Geddes, R.; Greenwood, G. T.; Jones, I. G. *Starch* **1972**, *24*, 245.
(27) Gidley, M. G. *Carbohydr. Res.* **1987**, *161*, 301−304.
(28) Glauert, A. M. *Fixation, Dehydration and Embedding of Biological Specimens*; 1987.
(29) Bram, A.; Branden, C. I.; Craig, C.; Snigireva, I.; Riekel, C. *J. Appl.Crystallogr.*, in press.
(30) Stroud, W. J.; Millane, R. P. *Acta Crystallogr.* **1995**, *A51*, 771−790.
(31) Stroud, W. J.; Millane, R. P. *Acta Crystallogr.* **1995**, 790−800.
(32) Stroud, W. J.; Millane, R. P. *Proc. R. Soc. London A* **1996**, *452*, 151−173.
(33) Riekel, C.; Bosecke, P.; Diat, O.; Lorenzen, M.; Sanchez del Rio, M.; Snigireva, I. *Rev. Sci. Instrum.* **1995**, *66*, 987−994.
(34) Unpublished small angle X-ray scattering data obtained on station 8.2 at Daresbury Laboratory, Warrington, England.
(35) Inouye, H. *Acta. Crystallogr.* **1994**, *A50*, 644−646.

MA970075W